Curr Radiol Rep (2017) 5:54
DOI 10.1007/s40134-017-0240-x

PEDIATRICS (L AVERILL, SECTION EDITOR)

MR Imaging of the Fetal Chest and Abdomen: How to Provide Value-Added Imaging

Eva Ilse Rubio[1,2,3]

Published online: 19 August 2017

Abstract
Purpose of Review In this article, recent literature on MRI of the fetal chest and abdomen is presented, with review of the growing area of fetal interventions. Emerging imaging techniques, the increasing trend toward 3 T in fetal imaging, as well as imaging protocols designed to optimize efficient evaluation of specific disease conditions will be discussed.
Recent Findings Prenatal MRI has been shown to contribute to accurate diagnoses of intrapulmonary lesions, and is anticipated to play an increasingly important role in cardiac disease. While the role of prenatal MRI in evaluation of the fetus with congenital diaphragmatic hernia is well known, there is now more concise information available in predicting postnatal outcomes; it plays a central role in planning and assessment of fetoscopic endoluminal tracheal occlusion (FETO). Complex congenital abdominal abnormalities also benefit from multiplanar imaging and the ability to delineate meconium distribution.
Summary MRI contributes meaningfully to evaluation of the fetus, providing information beyond what is obtained from advanced ultrasound (US). This allows for more nuanced prenatal counseling, a tailored multidisciplinary approach to prenatally diagnosed diseases and improved postnatal management.

Keywords Congenital diaphragmatic hernia · Congenital pulmonary airway malformation · Congenital high airway obstruction syndrome · Omphalocele · Gastroschisis · Limb-body wall complex

Introduction

The use of MRI in prenatal imaging emerged in the early 1990s with the advent of faster sequences and paralleled the development of fetal therapeutic interventions. Early imaging focused on maternal and placental pathology, and over time the utility of MRI for myriad other conditions became apparent [1•]. Although US remains the primary tool for screening, and diagnosis in many cases, the inherent soft tissue contrast of MRI can provide further detailed information in many diagnoses. However, valid questions are often posed about the potential overuse of the modality in some conditions. The value of MRI in evaluation of the fetus, with particular attention to how MRI facilitates prenatal diagnosis and management beyond what US offers, will be the focus of this article.

Technical Considerations

Many centers are performing prenatal imaging with a 1.5 T magnet; however increasing experience with 3 T both in Europe and in the United States has resulted in development of effective techniques to decrease artifacts associated with 3 T as well as optimization of the advantages of imaging at higher magnet strengths, which include

This article is part of the Topical collection on *Pediatrics*.

✉ Eva Ilse Rubio
erubio@childrensnational.org

[1] Department of Radiology, Children's National Health System, 111 Michigan Avenue NW, Washington, DC 20010, USA

[2] Division of Diagnostic Imaging and Radiology, Children's National Medical Center, Washington, DC, USA

[3] George Washington School of Medicine, Washington, DC, USA

increased signal to noise, higher image quality and decreased acquisition time [1•]. Additionally, many centers are transitioning to 3 T imaging out of necessity and equipment availability. Whether the advantages noted above or the thinner slices of 3 T imaging will result in greater accuracy in fetal thoracoabdominal imaging remains to be seen [2].

Protocols

Some centers approach fetal imaging in a more targeted fashion, focusing on the primary abnormality, and commenting on other parts of the fetus incidentally imaged. Other centers take a more comprehensive approach, with complete imaging and reporting on the entire fetus. Both approaches have their merits; a balance must be struck among available resources, including magnet time, radiologist availability, and local preferences of referring providers. In either setting, developing imaging protocols for common diagnoses is helpful for consistency in studies.

Evaluation of the Fetal Thorax

Normal Lung Tissue

Normal fetal lungs grow rapidly in the latter part of the second and throughout the third trimester, with an average fetal lung volume of 26.15 mL between 21 and 25 weeks gestation and 77.5 mL between 35.5 and 38 weeks gestation; the range of normal lung volume values also increases toward the end of pregnancy, with the lower and upper values at 38 weeks established as 38 and 150 mL, respectively [3]. Normal fetal lung tissue increases in its T2 signal intensity as the pregnancy progresses, as the parenchyma matures and the tissue accumulates fluid; this observation is most conspicuous in the third trimester [4]. In addition, the overall appearance of normal fetal lung tissue becomes increasingly heterogeneous, a consideration which should taken into account as late gestation lung lesions are evaluated (Fig. 1).

Achieving consistency in technique when measuring fetal lung volumes by MRI is important for accurate utilization of normative data and generation of the various percentages and ratios listed below in the setting of congenital diaphragmatic hernia. Within a group of fetal radiologists, it is also helpful to standardize technique among the readers so the clinicians can counsel patients at that center consistently. Slice thickness on T2-weighted images is often optimally 3–4 mm and there should be no gap or overlap; sequences often have to be repeated if there is excessive motion. Attention to how the lines are drawn around the hila and thymus, particularly later in gestation when the thymus is more conspicuous, will facilitate having a unified approach (Fig. 2). Once obtained, observed lung volumes are often used to calculate observed/expected total fetal lung volumes (O/E TFLV) by utilizing a formula based on gestational age to obtain the expected volume for age [3]. Establishing consistency in obtaining lung-to-head (LHR) ratios by US is likewise important, and often challenging.

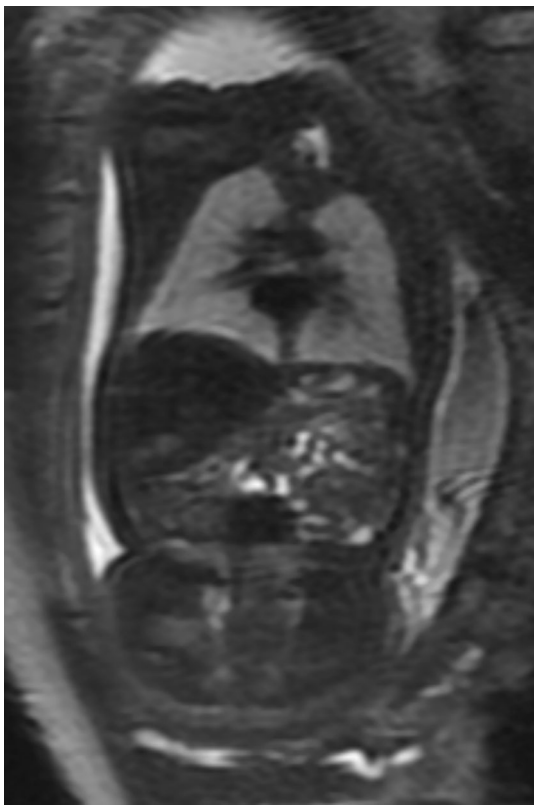

Fig. 1 Coronal image of a 30-week fetus; note mild heterogeneity of the lungs as well as small amounts of fluid in central bowel loops, normal findings at this gestational age

Lung Lesions

Intrapulmonary lesions most commonly encountered in fetal imaging practice include congenital pulmonary airway malformations (CPAM), bronchopulmonary sequestrations (BPS), hybrid lesions which contain elements of the two prior entities, congenital overinflation (CO) and cysts. The need for MRI in these cases remains a matter of debate. The congenital cystic adenomatoid malformation volume ratio (CVR), obtained by dividing a lesion's volume determined with US measurements by the head circumference, is a common method of assessing the severity of a lesion and the likelihood of developing hydrops [5]. One study of 52 cases found that MRI alone was highly

Fig. 2 *Arrowheads* indicate lines drawn manually around *right* and *left* lungs in this fetus with a CDH to obtain lung volumes

accurate in establishing the correct diagnosis in a spectrum of different lung lesions (>90%) with the most common being CPAM which are estimated to constitute 30–40% of all lung lesions [6] (Fig. 3). However, MRI is not the first line of imaging in pregnancy. A separate study comparing US and MRI in 22 cases of a spectrum of lung lesions found that US and MRI were generally equivalent in their ability to secure the correct diagnosis, although each modality had its own advantages: US was better able to delineate the feeding vessel in BPS while MRI better demonstrated cysts and margins with normal tissue [7].

There is increasing awareness of the entity CO, a lesion resulting from intrinsic or extrinsic bronchial obstruction causing alveolar overexpansion, previously considered rare but now recognized more commonly with improved imaging techniques; one study of 25 cases of prenatal CO found that these lesions represented 17% of all fetal lung lesions at a single center over a 7 year period [8]. This study also described the typical imaging features of CO, including a homogeneous T2 bright lesion commonly presenting with a central fluid-filled tubular structure near the hilum, and notable absence of pulmonary vasculature distortion. The latter imaging features were better seen by MRI. While many lesions are asymptomatic after birth and may be managed conservatively, CO lesions with central high grade obstruction were found to be at higher risk of morbidity and mortality.

Anticipating neonatal respiratory distress is a central goal of prenatal imaging. Lesions range from small and asymptomatic to massive, filling nearly the entire thorax. In a study of 47 prenatal lung masses, it was found that the strongest predictors of neonatal respiratory compromise and need for intubation, ECMO or surgery were a maximal lesion volume of 24 mL as measured by MRI and 34 mL by US [9]. In the third trimester, the increasingly heterogeneous appearance of maturing lungs may make distinguishing known intrapulmonary pulmonary lesions from normal lung tissue difficult.

Congenital Diaphragmatic Hernia

Congenital diaphragmatic hernia is a defect of unknown etiology which is estimated to affect approximately 1 in 3000–4000 live births [10]. Myriad methods of assessment, measurement and ratios have been developed over the years to predict mortality and morbidity, including the likelihood of developing chronic lung disease, pulmonary hypertension, and the need for extracorporeal membrane oxygenation

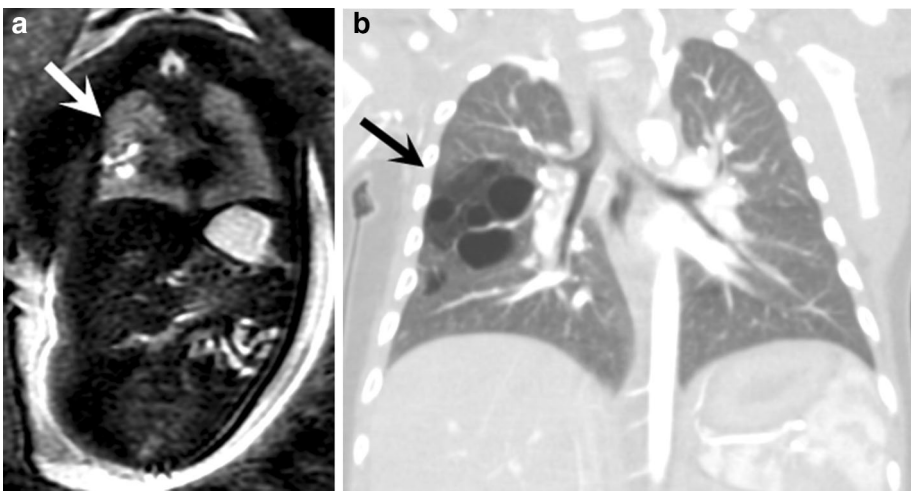

Fig. 3 **a** Clustered cystic foci are seen in the right mid lung (*arrow*) in this 30-week fetus consistent with a CPAM. **b** Postnatal coronal CT image of the same patient at 3 months of age. *Arrow* indicates the lesion

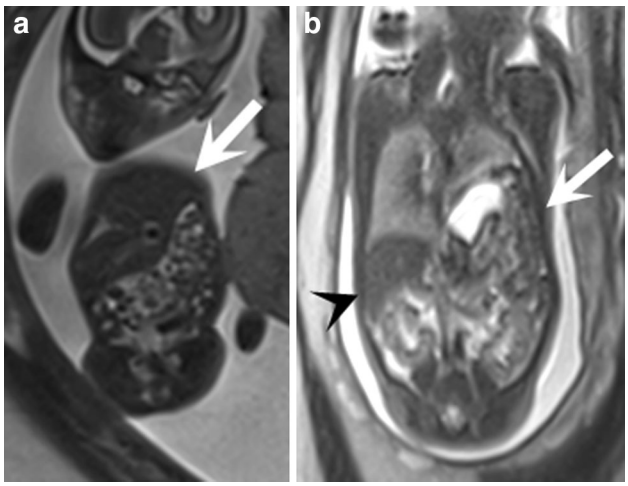

Fig. 4 **a** Large CDH in a 21-week fetus with liver herniated into the thorax (*arrow*). **b** Coronal image of a 25-week fetus with a left CDH containing bowel and stomach (*arrow*); the liver (*arrowhead*) remains within the abdomen

(ECMO), or patch repair (Fig. 4). These measurements include the lung-to-head ratio (LHR), observed/expected LHR (O/E LHR), percent predicted lung volume (PPLV), liver position, total lung volume (TLV), observed/expected total fetal lung volume (O/E TFLV), percentage liver herniation, prenatal pulmonary hypertension index (PPHI) and modified McGoon index (MGI) [11–18]. In addition, a congenital diaphragmatic hernia congenital prognostic index (CDH-CPI) which incorporates many of these factors, in addition to karyotype analysis and echocardiogram findings, has been developed to facilitate stratification of patients with this disease [19]. MRI calculation of prenatal lung volumes in fetuses with CDH is nearly universal among fetal care centers and is considered a important part of establishing the severity of disease. Patients with CDH have been stratified into low- and high-risk categories based on O/E TFLV, with the low risk group defined as those with greater than 35% O/E TFLV while those with an O/E TFLV less than 35% comprised the high-risk group: this system predicted a greater likelihood of requiring ECMO, needing additional support at 30 DOL, developing pulmonary hypertension and an overall lower survival in the high-risk group [16]. Further analysis confirmed O/E TFLV of <35% as an independent predictor of 6-month mortality, calculated at 44% [20•]. O/E FLV of the lung contralateral to the defect alone has also been established as a predictor of survival, need for ECMO and development of CLD: all patients with an O/E MR FLV below 18.3% expired while those above 53.5% survived [21]. There is increasing attention paid to both liver position and the percentage of liver herniated into the chest in assessing these patients; a cut-off value of greater than 20% of total liver tissue herniation into the chest predicted a higher likelihood of chronic lung disease, pulmonary hypertension and need for ECMO [16]. The mortality rate associated with more than 20% liver herniation into the chest is calculated at 36% [20•]. The likelihood of postnatal CDH repair with a prosthetic patch has also been described: patients with prenatal O/E FLV lower than 27.7% and liver herniation into the chest were substantially more likely to require patch repair [22]. In the same study this also correlated with a higher need for ECMO. It should be noted that right-sided CDH, which compose a minority of all CDH cases, often do not follow the same prognostic patterns as left-sided defects; typical cut-off values applied to left CDH in predicting severity do not clearly extrapolate to right CDH cases [23].

Fetoscopic Endoluminal Tracheal Occlusion (FETO)

In cases where a fetus carries a diagnosis of a severe isolated left CDH (L-CDH), this emerging procedure, which entails transabdominal access to the fetus via fetoscopy, placement of a detachable balloon into the fetal trachea to stimulate lung growth via fluid entrapment, and subsequent removal of the balloon after a period of weeks, may be offered; the procedure is generally performed between 22 and 32 weeks gestational age and centers offering the procedure typically require the mother to remain near the medical facility in the event of early onset delivery [24, 25, 26•, 27] (Fig. 5). The tracheal balloon is retrieved after several weeks as part of a second fetoscopic procedure. A severe L-CDH is typically characterized as one in which the O/E LHR is <35%, with liver herniated into the thorax [25, 26•, 27]. Multiple studies have demonstrated substantial improvements in survival, pulmonary hypertension, and need for ECMO in patients in the severe L-CDH category who underwent FETO procedure, when compared with similar cases in which FETO was not performed [25, 26•]. Specific survival rates depend on the center, protocols, techniques, and experience; survival rates of patients who underwent FETO range from 46 to 80%, vs 4.6 to 11% of patients with similarly severe L-CDH who did not [24, 25, 26•]. Preterm premature rupture of membranes, premature delivery, and intra-amniotic hemorrhage have been reported complications [24].

Cardiac MRI

The role of MRI in evaluation of fetal cardiac anomalies is gaining acceptance; in addition to its large field of view and tissue contrast, MRI has advantages in cases of oligohydramnios, large maternal body habitus, twin pregnancies, and late gestation larger fetuses. In one study of 68 patients, the diagnostic sensitivity of fetal cardiac MRI approached that of echocardiography, and in 10 cases findings were missed or misdiagnosed by echocardiography but correctly diagnosed by MRI; examples included

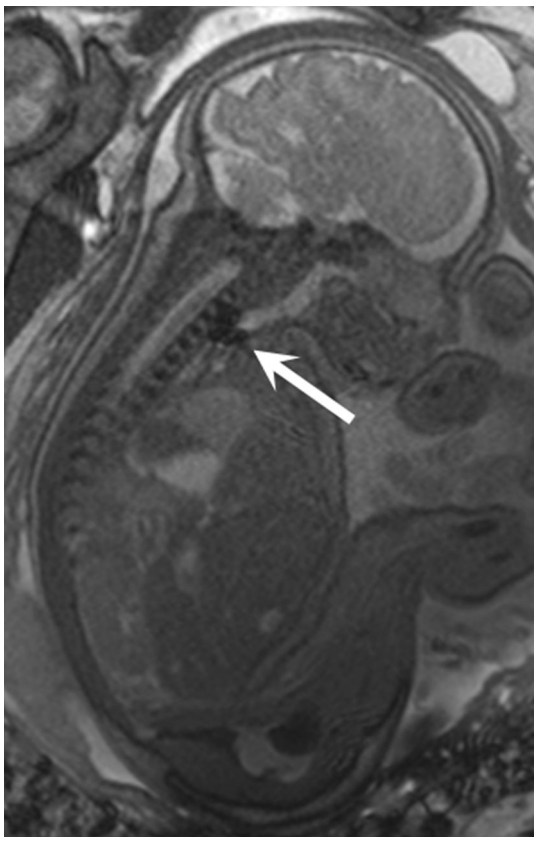

Fig. 5 Sagittal HASTE image of a fetus with an isolated L-CDH and FETO balloon in place in the trachea (*arrow*)

interrupted IVC, double outlet right ventricle and double aortic arch. Imaging protocols utilized include steady-state free-precession (SSFP) sequences, real-time SSFP, and single-shot turbo spin echo (SSTSE) [28]. Imaging protocols may benefit from overlapping of sequential slices. The utility of MRI as important adjunct imaging in assessing abnormalities of cardiac axis has also been studied: in one series of 42 cases, the etiology for cardiac malposition was reassigned in 29% of cases after MRI was performed [29]. The superiority in identifying persistent left superior vena cava (LSVC) has also been demonstrated; in one series of 49 fetuses, all cases of persistent LSVC were seen by MRI although 15 were not identified by prenatal US and/or echocardiography. The significance of this finding lies in its strong association with both cardiac and extra cardiac abnormalities [30] (Fig. 6).

Nutmeg Lung

An entity which may be infrequently encountered has been described as "nutmeg lung", a pattern of diffuse parenchymal heterogeneity with branching fluid-filled tubules emanating from the hila and pleural effusions; the appearance may represent primary or secondary lymphangiectasia and should be recognized as a potential sign of cardiac or respiratory insufficiency [31]. It has also been described as a particularly poor prognostic indicator when seen in a fetus with hypoplastic left heart syndrome [32] (Fig. 7).

Evaluation of the Fetal Abdomen

Imaging Approach and Protocols

Utilization of MRI in evaluation of fetal abdominal abnormalities is generally undertaken to assess bowel obstruction, solid tumors, or cystic lesions. Imaging characteristics of abdominal pathology as depicted by T2-weighted and T1 images often yield helpful information in securing a diagnosis; US provides significant useful information as well, and remains superior to MRI in depiction of calcification. Abdominal imaging protocols should include both T1- and T2-weighted sequences in at least two planes; T1-weighted

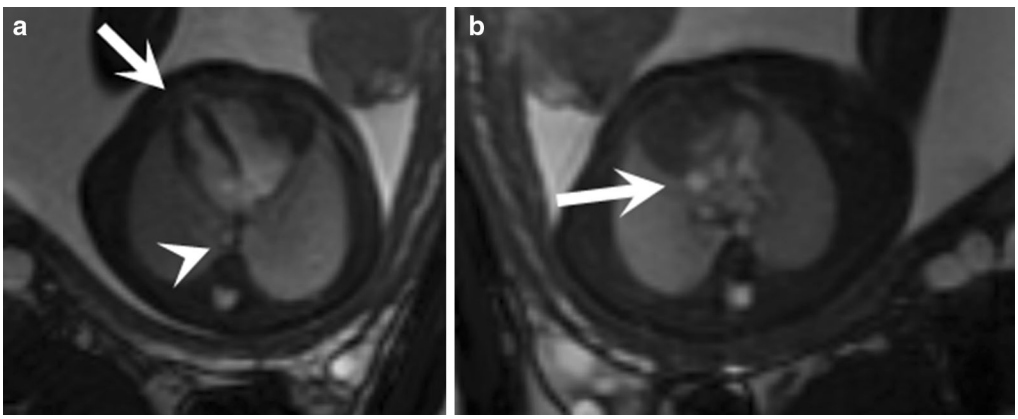

Fig. 6 **a** Axial SSFP image of the fetal heart at 30 weeks gestation; the *arrow* indicates the cardiac apex and the *arrowhead* indicates the descending aorta, both *left-sided*. **b** Axial image demonstrates the 3-vessel view equivalent: pulmonary outflow tract, aorta and superior vena cava (*arrow*)

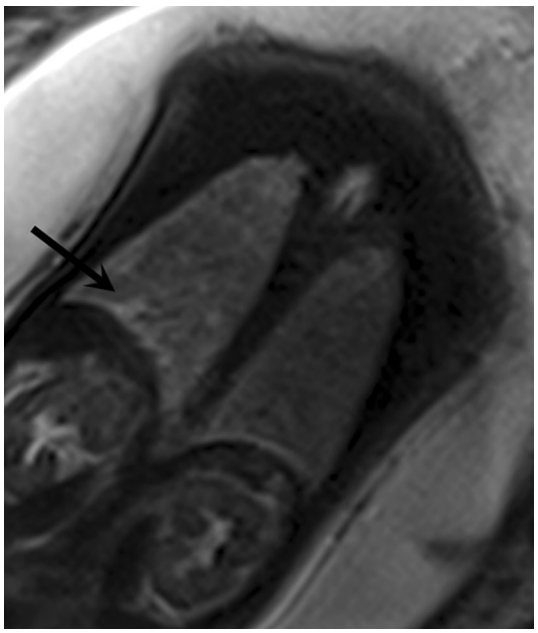

Fig. 7 Coronal image of the lungs in this 32-week fetus demonstrates the appearance of "nutmeg lung": heterogeneous parenchyma, trace effusions and high signal intensity radiating tubules (*arrow*) in this patient with hypoplastic left heart

imaging in the sagittal plane optimally depicts the position of the fetal rectum relative to the bladder; the distal rectal column should terminate 5-10 mm below the level of the base of the urinary bladder to confidently exclude an anorectal malformation. Meconium is first expected to appear in the fetal rectum at 20 weeks gestation. T1-weighted slice thickness of 5 mm has been found to be suitable for fetuses of all gestational ages (Fig. 8).

Bowel Obstruction

Although fetal bowel obstruction is often evaluated prenatally by US alone, one study of 42 patients found that US and MRI combined had an overall accuracy of 84.4% in assessment of bowel obstruction; the highest rate of accuracy was in anorectal obstruction (100%), a category which also carried the highest rate of associated anomalies (90.1% of patients) and the lowest rate of survival (54.5%) [33].

In a separate study of 12 cases of jejunal and ileal obstruction, a trend of increasing complexity of bowel contents was demonstrated by both US and MRI with increasingly distal obstructive lesions (Fig. 9); other findings included diffusely thinned T1 meconium signal throughout the colon in all cases of small bowel obstruction, and near-complete or complete absence of rectal meconium in cases of cystic fibrosis. No definite signs to predict an outcome of short bowel syndrome were identified prenatally, however [34].

In a prospective study of 38 fetuses evaluated by US and MRI, MRI was found to provide additional information in

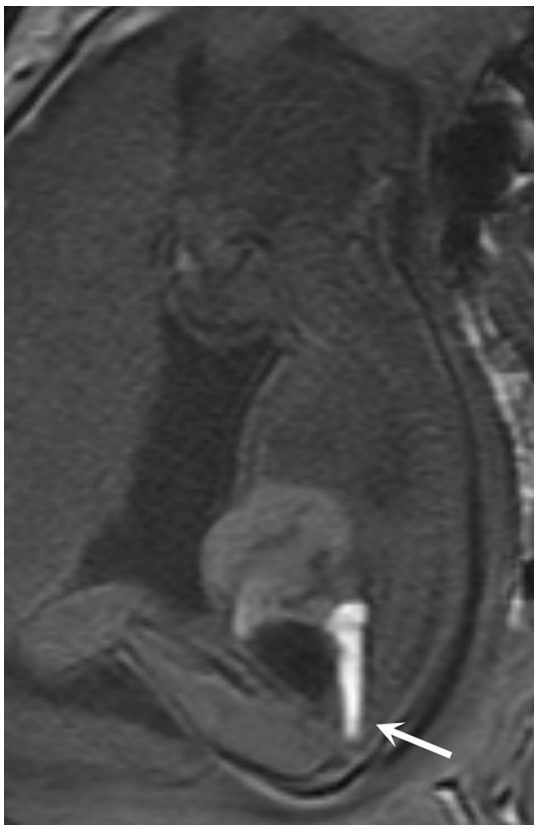

Fig. 8 *Arrow* indicates the position of the normal T1 bright meconium column, terminating *below* the base of the urinary bladder, in this 30-week fetus

60.6%, including the level of obstruction, clarification of meconium pseudocyst, and differentiation from massively dilated ureters [35].

Congenital Diarrhea

An uncommon diagnosis in the fetus is that of congenital diarrhea; while fluid-filled bowel loops can be clearly seen throughout the abdomen by US resembling a distal bowel obstruction, MRI is able to establish the diagnosis by confirming complete absence of the expected T1 bright meconium signal, owing to diffuse dilution with the high water content throughout [36].

Cystic Lesions

Evaluation of abdominal cystic lesions is a common indication for advanced imaging. A retrospective study of 49 cases of abdominal cystic lesions evaluated by both US and MRI found that MRI confirmed or corrected the US diagnosis in 73.4% of cases, rectifying the initial diagnosis in 26.5%, an advantage which was primarily appreciated in upper abdominal lesions [37].

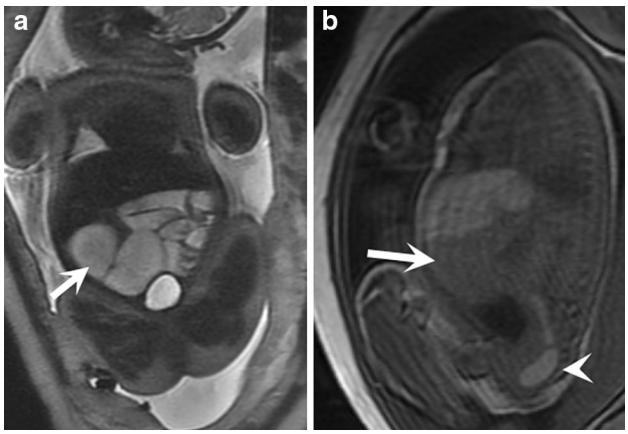

Fig. 9 **a** Coronal T2-weighted image of a 36 week fetus with jejunal atresia; *arrow* indicates dilated loops with mildly complex fluid contents. **b** Sagittal T1-weighted image of the same fetus; *arrow* indicates complex intraluminal fluid contents evidenced by intermediate T1 signal. In spite of the small bowel obstruction, a normally positioned meconium filled rectum is identified (*arrowhead*)

Abdominal Wall Defects

Anterior abdominal wall defects in the fetus may occur in the form of gastroschisis, omphalocele, bladder exstrophy, cloacal exstrophy, limb-body wall complex (LBWC), Pentalogy of Cantrell, and ectopia cordis [38]. Factors limiting imaging in these fetuses include maternal obesity, multiparity, fetal lie, and oligohydramnios; securing the correct prenatal diagnosis is imperative for counseling, pregnancy management and decisions, and delivery/post-delivery planning [39]. These defects are defined primarily by the location of the defect relative to the umbilical cord insertion site in the fetal abdomen and the specific diagnosis can often be determined by US, although MRI may contribute by confirming anatomic relationships.

Gastroschisis

The prevalence is estimated at 1–6 per 3000–10,000 births; the defect is typically right paraumbilical in location, with an intact umbilical cord insertion site [38]. Gastroschisis defects may be large and include small bowel and colon, and portions of the bladder. However, the extruded abdominal contents should not include liver, a finding which should prompt consideration of an alternative diagnosis such as a ruptured omphalocele. Gastroschisis often does not warrant evaluation by MRI, which contributes little to the diagnosis. Associated anomalies are rare [38].

Omphalocele

The prevalence is approximately 0.8–3.9 per 10,000 births, and the condition is associated with additional visceral, spine or genetic in as many as 74% of cases; the defect is characterized by extruded abdominal contents covered by a membranous sac, with the umbilical cord inserting at or near the apex [38]. Some defects are categorized as giant omphalocele, a designation with variable definitions although it is generally accepted that with a majority of the liver outside the abdomen the term giant should apply. In contrast to gastroschisis, omphalocele is associated with a risk for pulmonary hypoplasia due to thoracic distortion and narrowing, and impaired diaphragmatic motion, which are often seen with large defects. The utility of MRI in these patients is therefore twofold: it is useful in detecting other myriad defects seen in these patients, and also may be used to calculate lung volumes in anticipation of pulmonary hypoplasia or postnatal respiratory compromise. In one study, patients with prenatally diagnosed omphalocele, congenital diaphragmatic hernia or lung malformations with O/E TFLV of 40–60% had comparable need for ECMO, supplemental oxygen at 30 days of life and similar mortality rates [40]. In another study, fetuses with giant omphalocele were stratified into groups based on O/E TFLV; postnatally, the group with lung volumes equal to or $<$50% O/E TFLV had higher rates of prolonged ventilation, delayed oral intake, and longer hospitalization [41].

Bladder Exstrophy

This condition occurs in 1 in 10,000–50,000 live births and is more commonly seen in males [38, 42]. Associated anomalies are not expected with bladder exstrophy [38]. Although the diagnosis may be suspected by US, MRI has been recognized as a useful adjunct in providing additional anatomic information, as an important differential consideration in these patients is cloacal exstrophy. MRI findings include absent urinary bladder filling, a low position of the umbilical insertion site, and a low abdominal mass below the umbilicus [43]. The kidneys, ureters, amniotic fluid, and fetal lungs are generally normal; MRI offers the benefits of optimal visualization of these structures particularly in cases of difficult fetal lie or large maternal body habitus [42]. Most importantly, clear identification of normal distal hindgut structures with a normal position of the meconium-filled rectum and sigmoid colon, and visualization of the fetal spine without dysraphism, are optimally provided by MRI, allowing for exclusion of cloacal exstrophy [38, 42, 43].

Cloacal Exstrophy

Also known as OEIS (omphalocele, cloacal exstrophy, imperforate anus, and spinal defects), this rare and severe defect of the anterior abdominal wall occurs in approximately 1 in 250,000–400,000 live births; in contrast to

bladder exstrophy, it affects both sexes equally and is associated with multisystem anomalies [38, 42]. The diagnosis is often not fully appreciated by prenatal US, and may be confused with omphalocele or bladder exstrophy. [38, 44] In addition to the omphalocele, which may range from quite small to giant in size, the pelvic anatomy in cloacal exstrophy is complex, and findings vary from patient to patient: absent urinary bladder is universal, and other findings may include pelvic or cloacal cysts, dilated and ectopic ureters, ectopic and obstructed kidneys, hydrocolpos, split externalized lateralized hemi-bladder plates, externally prolapsed central segment of terminal ileum ("elephant trunk") and absence of a meconium-filled rectum and sigmoid, the final abnormality being an important clue to the diagnosis [44]. Spinal anomalies are often present, and many are skin covered; care should be taken to scrutinize the entirety of the spine as many patients have spinal anomalies at more than one level [44]. MRI is indispensible in delineating these and other anomalies in the fetus with suspected cloacal exstrophy (Fig. 10).

Limb-Body Wall Complex (LBWC)

This exceedingly rare defect of the ventral fetus is estimated to occur in 0.3–3.3 per 10,000 pregnancies, and is generally defined as having 2 of 3 major features: (1) exencephaly or encephalocele with facial clefts; (2) ventral defects of the abdomen and/or thorax, and (3) extremity anomalies [38]. In addition to massive extrusion of thoracoabdominal contents adherent to the placenta, there is often severely angulated scoliosis, hypoplastic thoraces and a short or absent umbilical cord [45]. Imaging in these cases can be challenging, due to markedly distorted anatomy (Fig. 11). The value of MRI in these cases lies in confirming the diagnosis, as LBWC is virtually uniformly lethal, and has been associated with significant maternal morbidity in cases of late or declined pregnancy termination [46].

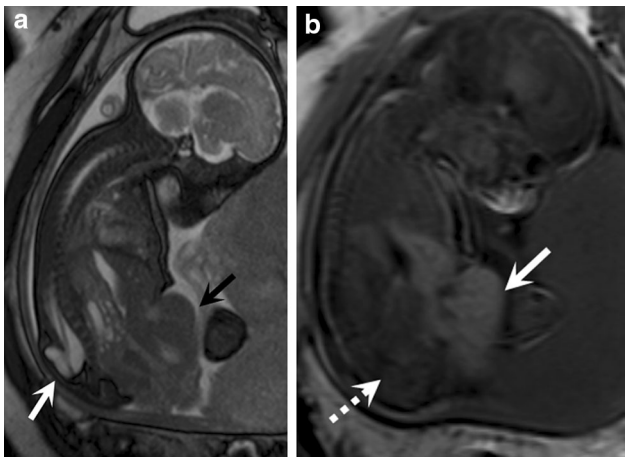

Fig. 10 **a** Sagittal SSFP image of a 30-week fetus with OEIS. There is a large omphalocele containing liver (*black arrow*) and skin-covered dysraphic defect of the sacral spine (*white arrow*). Note the absence of Chiari 2 malformation. **b** In the same fetus, T1-weighted sagittal imaging helps confirm the protruding liver (*solid arrow*) and absence of normal meconium-filled bowel in the expected region of the rectosigmoid (*dashed arrow*)

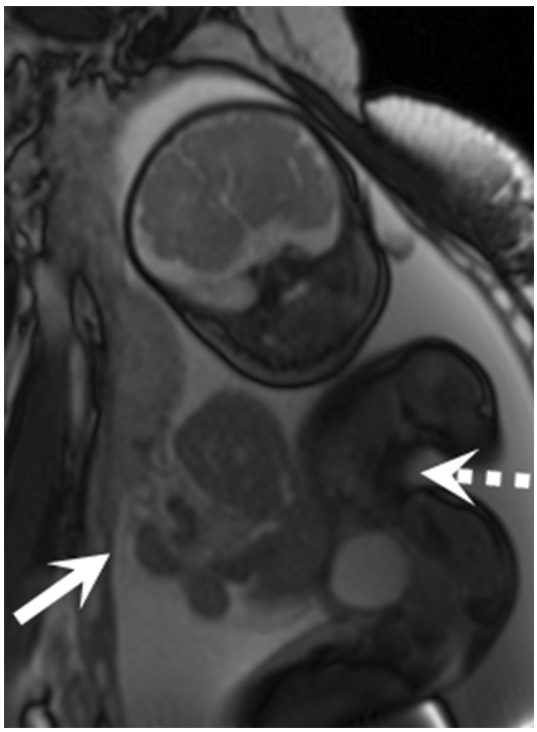

Fig. 11 Limb body wall complex: the white arrow demonstrates a large omphalocele with abdominal contents attached to the placenta (*solid arrow*). Severely angulated scoliosis (*dashed arrow*) makes planar imaging difficult

Conclusion

The role of MRI in evaluation of the fetus has expanded significantly since its inception; many studies have been able to demonstrate its contribution in establishing a more accurate, detailed diagnosis, and provide prognostic information in preparation for the neonatal period. Technologic advances and faster sequence acquisition time will allow for further advances in prenatal imaging.

Compliance with Ethical Guidelines

Conflict of Interest Eva Ilse Rubio declares no potential conflicts of interest.

Human and Animal Rights and Informed Consent This article does not contain any studies with human or animal subjects performed by any of the authors.

References

Papers of particular interest, published recently, have been highlighted as:
- • Of importance

1. • Victoria T, Jaramillo D, Roberts TP, Zarnow D, Johnson AM, Delgado J, Rubesova E, Vossough A. Fetal magnetic resonance imaging: jumping from 1.5 to 3 T (preliminary experience). Pediatr Radiol. 2014;44(4):376–86. *This article serves as a practical guide to anticipating and mitigating common prenatal imaging artifacts at 3 T; safety concerns are also addressed.*
2. Weisstanner C, Gruber GM, Brugger PC, Mitter C, Diogo MC, Kasprian G, Prayer D. Fetal MRI at 3 T-ready for routine use? Br J Radiol. 2017;90(1069):20160362.
3. Rypens F, Metens T, Rocourt N, Sonigo P, Brunelle F, Quere MP, Guibaud L, Maugey-Laulom B, Durand C, Avni FE, Eurin D. Fetal lung volume: estimation at MR imaging-initial results. Radiology. 2001;219(1):236–41.
4. Cannie M, Jani J, De Keyzer F, Roebben I, Breysem L, Deprest J. T2 quantifications of fetal lungs at MRI-normal ranges. Prenat Diagn. 2011;31(7):705–11.
5. Crombleholme TM, Coleman B, Hedrick H, Liechty K, Howell L, Flake AW, Johnson M, Adzick NS. Cystic adenomatoid malformation volume ratio predicts outcome in prenatally diagnosed cystic adenomatoid malformation of the lung. J Pediatr Surg. 2002;37(3):331–8.
6. Pacharn P, Kline-Fath B, Calvo-Garcia M, Linam LE, Rubio EI, Salisbury S, Brody AS. Congenital lung lesions: prenatal MRI and postnatal findings. Pediatr Radiol. 2013;43(9):1136–43.
7. Beydon N, Larroquet M, Coulomb A, Jouannic JM, Ducou le Pointe H, Clément A, Garel C. Comparison between US and MRI in the prenatal assessment of lung malformations. Pediatr Radiol. 2013;43(6):685–96.
8. Johnston JH, Kline-Fath BM, Bitters C, Calvo-Garcia MA, Lim FY. Congenital overinflation: prenatal MRI and US findings and outcomes. Prenat Diagn. 2016;36(6):568–75.
9. Girsen AI, Hintz SR, Sammour R, Naqvi A, El-Sayed YY, Sherwin K, Davis AS, Chock VY, Barth RA, Rubesova E, Sylvester KG, Chitkara R, Blumenfeld YJ. Prediction of neonatal respiratory distress in pregnancies complicated by fetal lung masses. Prenat Diagn. 2017;37(3):266–72.
10. Ackerman KG, Pober BR. Congenital diaphragmatic hernia and pulmonary hypoplasia: new insights from developmental biology and genetics. Am J Med Genet C Semin Med Genet. 2007;145C(2):105–8.
11. Lipshutz GS, Albanese CT, Feldstein VA, Jennings RW, Housley HT, Beech R, Farrell JA, Harrison MR. Prospective analysis of lung-to-head ratios predicts survival for patients with prenatally diagnosed congenital diaphragmatic hernia. J Pediatr Surg. 1997;32(11):1634–6.
12. Jani J, Nicolaides KH, Keller RL, Benachi A, Peralta CF, Favre R, Moreno O, Tibboel D, Lipitz S, Eggink A, Vaast P, Allegaert K, Harrison M, Deprest J, Deprest J. Observed to expected lung area to head circumference in the prediction of survival in fetuses with isolated diaphragmatic hernia. Ultrasound Obstet Gynecol. 2007;30(1):67–71.
13. Barnewolt CE, Kunisaki SM, Fauza DO, et al. Percent predicted lung volumes as measured on fetal magnetic resonance imaging: a useful biometric parameter for risk stratification in congenital diaphragmatic hernia. J Pediatr Surg. 2007;42:193–7.
14. Hedrick HL, Danzer E, Merchant A, et al. Liver position and lung-to-head ratio for prediction of extracorporeal membrane oxygenation and survival in isolated left congenital diaphragmatic hernia. Am J Obstet Gynecol. 2007;197(422):e1–4.
15. Lee TC, Lim FY, Keswani SG, et al. Late gestation fetal magnetic resonance imaging-derived total lung volume predicts postnatal survival and need for extracorporeal membrane oxygenation support in isolated congenital diaphragmatic hernia. J Pediatr Surg. 2011;46:1165–71.
16. Zamora IJ, Olutoye OO, Cass DL, Fallon SC, Lazar DA, Cassady CI, Mehollin-Ray AR, Welty SE, Ruano R, Belfort MA, Lee TC. Prenatal MRI fetal lung volumes and percent liver herniation predict pulmonary morbidity in congenital diaphragmatic hernia (CDH). J Pediatr Surg. 2014;49(5):688–93.
17. Nawapun K, Eastwood M, Sandaite I, DeKoninck P, Claus F, Richter J, Rayyan M. Deprest J Correlation of observed-to-expected total fetal lung volume with intrathoracic organ herniation on magnetic resonance imaging in fetuses with isolated left-sided congenital diaphragmatic hernia. Ultrasound Obstet Gynecol. 2015;46(2):162–7.
18. Vuletin JF, Lim FY, Cnota J, et al. Prenatal pulmonary hypertension index: novel prenatal predictor of severe postnatal pulmonary artery hypertension in antenatally diagnosed congenital diaphragmatic hernia. J Pediatr Surg. 2010;45:703–8.
19. Le LD, Keswani SG, Biesiada J, Lim FY, Kingma PS, Haberman BE, Frischer J, Habli M, Crombleholme TM. The congenital diaphragmatic hernia composite prognostic index correlates with survival in left-sided congenital diaphragmatic hernia. J Pediatr Surg. 2012;47(1):57–62.
20. • Akinkuotu AC, Cruz SM, Abbas PI, Lee TC, Welty SE, Olutoye OO, Cassady CI, Mehollin-Ray AR, Ruano R, Belfort MA, Cass DL. Risk-stratification of severity for infants with CDH: Prenatal versus postnatal predictors of outcome. J Pediatr Surg. 2016;51(1):44–8. *In this large cohort of CDH patients, major risk factors and risk stratification are reviewed, with postnatal outcome data.*
21. Hagelstein C, Burger-Scheidlin S, Weis M, Weiss C, Schoenberg SO, Schaible T, Neff KW. separate evaluation of the ipsilateral and contralateral MR fetal lung volume in patients with congenital diaphragmatic hernia. AJR Am J Roentgenol. 2016;207(2):415–23.
22. Hagelstein C, Zahn K, Weidner M, Weiss C, Schoenberg SO, Schaible T, Büsing KA, Neff KW. Prenatal MR imaging of congenital diaphragmatic hernias: association of MR fetal lung volume with the need for postnatal prosthetic patch repair. Eur Radiol. 2015;25(1):258–66.
23. Victoria T, Danzer E, Oliver ER, Edgar JC, Iyoob S, Partridge EA, Johnson AM, Peranteau WH, Coleman BG, Flake AW, Johnson MP, Hedrick HH, Adzick NS. Right congenital diaphragmatic hernias: is there a correlation between prenatal lung volume and postnatal survival, as in isolated left diaphragmatic hernias? Fetal Diagn Ther. 2017;. doi:10.1159/000464246.
24. Ruano R, Ali RA, Patel P, Cass D, Olutoye O, Belfort MA. Fetal endoscopic tracheal occlusion for congenital diaphragmatic hernia: indications, outcomes, and future directions. Obstet Gynecol Surv. 2014;69(3):147–58.
25. Al-Maary J, Eastwood MP, Russo FM, Deprest JA, Keijzer R. Fetal tracheal occlusion for severe pulmonary hypoplasia in isolated congenital diaphragmatic hernia: a systematic review and meta-analysis of survival. Ann Surg. 2016;264(6):929–33.
26. • Belfort MA, Olutoye OO, Cass DL, Olutoye OA, Cassady CI, Mehollin-Ray AR, Shamshirsaz AA, Cruz SM, Lee TC, Mann DG, Espinoza J, Welty SE, Fernandes CJ, Ruano R. Feasibility and Outcomes of Fetoscopic Tracheal Occlusion for Severe Left Diaphragmatic Hernia. Obstet Gynecol. 2017;129(1):20–9. *This article compares a prospective cohort of treated patients with*

historical controls; a comprehensive discussion of protocols, patient selection, the procedure and outcomes is included.
27. Ali K, Bendapudi P, Polubothu S, Andradi G, Ofuya M, Peacock J, Hickey A, Davenport M, Nicolaides K, Greenough A. Congenital diaphragmatic hernia-influence of fetoscopic tracheal occlusion on outcomes and predictors of survival. Eur J Pediatr. 2016;175(8):1071–6.
28. Dong SZ, Zhu M, Li F. Preliminary experience with cardiovascular magnetic resonance in evaluation of fetal cardiovascular anomalies. J Cardiovasc Magn Reson. 2013;15:40.
29. Gaur L, Talemal L, Bulas D, Donofrio MT. Utility of fetal magnetic resonance imaging in assessing the fetus with cardiac malposition. Prenat Diagn. 2016;36(8):752–9.
30. Dong SZ, Zhu M. Magnetic resonance imaging of fetal persistent left superior vena cava. Sci Rep. 2017;7(1):4176.
31. Victoria T, Andronikou S. The fetal MR appearance of 'nutmeg lung': findings in 8 cases linked to pulmonary lymphangiectasia. Pediatr Radiol. 2014;44(10):1237–42.
32. Saul D, Degenhardt K, Iyoob SD, Surrey LF, Johnson AM, Johnson MP, Rychik J, Victoria T. Hypoplastic left heart syndrome and the nutmeg lung pattern in utero: a cause and effect relationship or prognostic indicator? Pediatr Radiol. 2016;46(4):483–9.
33. Lau PE, Cruz S, Cassady CI, Mehollin-Ray AR, Ruano R, Keswani S, Lee TC, Olutoye OO, Cass DL. Prenatal diagnosis and outcome of fetal gastrointestinal obstruction. J Pediatr Surg. 2017;52(5):722–5.
34. Rubio EI, Blask AR, Badillo AT, Bulas DI. Prenatal magnetic resonance and ultrasonographic findings in small-bowel obstruction: imaging clues and postnatal outcomes. Pediatr Radiol. 2017;47(4):411–21.
35. Manganaro L, Saldari M, Bernardo S, Vinci V, Aliberti C, Sollazzo P, Giancotti A, Capozza F, Porpora MG, Cozzi DA, Catalano C. Role of magnetic resonance imaging in the prenatal diagnosis of gastrointestinal fetal anomalies. Radiol Med. 2015;120(4):393–403.
36. Colombani M, Ferry M, Toga C, Lacroze V, Rubesova E, Barth RA, Cassart M, Gorincour G. Magnetic resonance imaging in the prenatal diagnosis of congenital diarrhea. Ultrasound Obstet Gynecol. 2010;35(5):560–5.
37. Hugele F, Dumont C, Boulot P, Couture A, Prodhomme O. Does prenatal MRI enhance fetal diagnosis of intra-abdominal cysts? Prenat Diagn. 2015;35(7):669–74.
38. Torres US, Portela-Oliveira E, Braga Fdel C, Werner H Jr, Daltro PA, Souza AS. When closure fails: what the radiologist needs to know about the embryology, anatomy, and prenatal imaging of ventral body wall defects. Semin Ultrasound CT MR. 2015;36(6):522–36.
39. Nakagawa M, Hara M, Shibamoto Y. MRI findings in fetuses with an abdominal wall defect: gastroschisis, omphalocele, and cloacal exstrophy. Jpn J Radiol. 2013;31(3):153–9.
40. Akinkuotu AC, Sheikh F, Cass DL, Zamora IJ, Lee TC, Cassady CI, Mehollin-Ray AR, Williams JL, Ruano R, Welty SE, Olutoye OO. Are all pulmonary hypoplasias the same? A comparison of pulmonary outcomes in neonates with congenital diaphragmatic hernia, omphalocele and congenital lung malformation. J Pediatr Surg. 2015;50(1):55–9.
41. Danzer E, Victoria T, Bebbington MW, Siegle J, Rintoul NE, Johnson MP, Flake AW, Adzick NS, Hedrick HL. Fetal MRI-calculated total lung volumes in the prediction of short-term outcome in giant omphalocele: preliminary findings. Fetal Diagn Ther. 2012;31(4):248–53.
42. Chauvin NA, Epelman M, Victoria T, Johnson AM. Complex genitourinary abnormalities on fetal MRI: imaging findings and approach to diagnosis. AJR Am J Roentgenol. 2012;199(2):W222–31.
43. Goldman S, Szejnfeld PO, Rondon A, Francisco VV, Bacelar H, Leslie B, Barroso U Jr, Ortiz V, Macedo A Jr. Prenatal diagnosis of bladder exstrophy by fetal MRI. J Pediatr Urol. 2013;9(1):3–6.
44. Calvo-Garcia MA, Kline-Fath BM, Rubio EI, Merrow AC, Guimaraes CV, Lim FY. Fetal MRI of cloacal exstrophy. Pediatr Radiol. 2013;43(5):593–604.
45. Aguirre-Pascual E, Epelman M, Johnson AM, Chauvin NA, Coleman BG, Victoria T. Prenatal MRI evaluation of limb-body wall complex. Pediatr Radiol. 2014;44(11):1412–20.
46. Costa ML, Couto E, Furlan E, Zaccaria R, Andrade K, Barini R, Nomura ML. Body stalk anomaly: adverse maternal outcomes in a series of 21 cases. Prenat Diagn. 2012;32(3):264–7.